

## Structural Characteristics around the $\beta$ -Ionone Ring of the Retinal Chromophore in *Salinibacter* Sensory Rhodopsin I

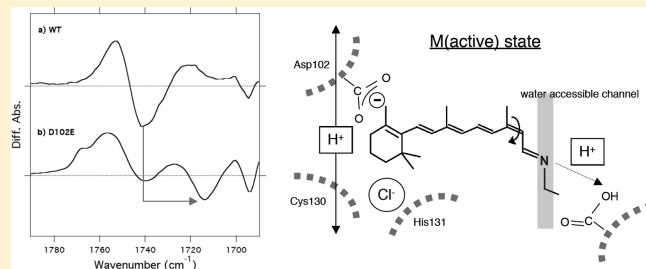
Hiroki Irieda,<sup>†,‡</sup> Louisa Reissig,<sup>†,‡</sup> Akira Kawanabe,<sup>‡</sup> Michio Homma,<sup>†</sup> Hideki Kandori,<sup>‡</sup> and Yuki Sudo<sup>\*,†,§</sup>

<sup>†</sup>Division of Biological Science, Graduate School of Science, Nagoya University, Nagoya 464-8602, Japan

<sup>‡</sup>Department of Frontier Materials, Nagoya Institute of Technology, Showa-ku, Nagoya 466-8555, Japan

<sup>§</sup>PRESTO, Japan Science and Technology Agency (JST), 4-1-8 Honcho Kawaguchi, Saitama 332-0012, Japan

**ABSTRACT:** Organisms sense and respond to environmental stimuli through membrane-embedded receptors and transducers. Sensory rhodopsin I (SRI) and sensory rhodopsin II (SRII) are the photoreceptors for the positive and negative phototaxis in microorganisms, respectively. They form signaling complexes in the membrane with their cognate transducer proteins, HtrI and HtrII, and these SRI–HtrI and SRII–HtrII complexes transmit a light signal through their cytoplasmic sensory signaling system, inducing opposite effects (i.e., the inactivation or activation of the kinase CheA). Here we found, by using Fourier transformed infrared spectroscopy, that a conserved residue, Asp102 in *Salinibacter* SRI (SrSRI), which is located close to the  $\beta$ -ionone ring of the retinal chromophore, is deprotonated upon formation of the active M-intermediate. Furthermore, the D102E mutant of SrSRI affects the structure and/or structural changes of Cys130. This mutant shows a large spectral shift and is comparably unstable, especially in the absence of  $\text{Cl}^-$ . These phenomena have not been observed in the wild-type, or the N105Q and N105D mutants of *Natronomonas pharaonis* SRII (*NpSRII*), indicating differences in the structure and structural changes between SrSRI and *NpSRII* around the  $\beta$ -ionone ring. These differences could also be supported by the measurements of the reactivity with the water-soluble reagent azide. On the basis of these results, we discuss the structure and structural changes around the retinal chromophore in SrSRI.



Motile microorganisms, such as bacteria and archaea, sense and respond to extracellular stimuli by changing their swimming mode to migrate toward more favorite habitats. This behavior, termed *taxis*, is achieved by a signaling system from membrane-embedded receptors (input) to the flagellar motor (output) (for reviews, see refs 1–4). Microorganisms have two distinct swimming modes, run (smooth swimming) and reorientation (tumbling, slowing down, stopping, switching, etc.), resulting in the change of direction of the flagellar motor rotation. To seek optimal locations, microorganisms control the activity of the histidine kinase CheA and modulate the reorientation frequency. An attractive and a repellent stimulation decreases (positive signaling) or increases (negative signaling) the kinase activity, respectively.

Sensory rhodopsins (SRs) are seven-transmembrane photosensors containing retinal (vitamin A aldehyde) as a chromophore and are widespread in the microbial world.<sup>2,4</sup> Sensory rhodopsin I (SRI) and sensory rhodopsin II (SRII) form 2:2 signaling complexes with their two-transmembrane cognate halobacterial transducer proteins, HtrI and HtrII, respectively.<sup>5,6</sup> The cytoplasmic tip of these Htrs is believed to interact with CheA via an adaptor protein, CheW,<sup>4</sup> as well as the well-studied bacterial chemoreceptors, Tar and Tsr.<sup>1</sup> Depending on the color of the light the quaternary complex of SR-Htr-CheW-CheA can mediate a phototaxis response.<sup>2,7</sup> SRI and SRII are responsible

for the positive and negative phototaxis, respectively.<sup>2</sup> Furthermore, SRI is also able to work as a negative phototaxis receptor by a two-photon photoreaction.<sup>7</sup> In the case of SRI from *Halobacterium salinarum* (*HsSRI*), the ground state (absorption maximum,  $\lambda_{\max}$  of 587 nm) is essential for the positive phototaxis, while the signaling state (long-lived M-intermediate,  $\lambda_{\max}$  of 373 nm) induces the negative phototaxis. In contrast, in the case of SRII from *H. salinarum*, only the ground state ( $\lambda_{\max}$  of 487 nm) can generate a negative phototaxis response.<sup>8</sup> By using the sensory system, *H. salinarum* cells are attracted to light whose wavelengths are longer than 520 nm, while light of shorter wavelengths is avoided. This is essential, as light of  $\lambda > 520$  nm can activate ion pumping rhodopsins, bacteriorhodopsin (BR)<sup>9</sup> and halorhodopsin (HR),<sup>10</sup> which enables the cells to obtain the energy from the light, while also avoiding harmful near-UV radiation.

The structure and structural changes of SRII have been well characterized over the past 10 years because of the high protein stability of SRII from the archaeon *Natronomonas pharaonis* (*NpSRII*).<sup>3,4,11</sup> The sixth and seventh transmembrane helices (F- and G-helices) of *NpSRII* interact with the first and second

**Received:** February 23, 2011

**Revised:** May 4, 2011

**Published:** May 05, 2011

transmembrane helices (TM1 and TM2) of *NpHtrII* in both the unphotolyzed and photoactivated states.<sup>6,12</sup> Two hydrogen bonds on the binding surface are involved in the specific interaction.<sup>13,14</sup> Upon formation of an active M-intermediate, the cytoplasmic part of helix-F of *NpSRII* moves outward, which causes a rotation of TM2 in HtrII.<sup>15,16</sup> This outward movement of helix-F of SRII is also supported by the increase in the reactivity with the water-soluble reagents, azide and hydroxylamine.<sup>17</sup> These conformational changes have been proposed to be important for the signal transduction.<sup>18</sup>

Compared to SRII, the signal relay mechanism of SRI is poorly characterized, although some characterization experiments have been performed.<sup>7</sup> This was mainly due to the instability of *HsSRI*, especially in dilute salt solutions.<sup>19</sup> Recently, we characterized a new SRI-like protein from the eubacterium *Salinibacter ruber* (*SrSRI*) as well as its complex with its cognate transducer protein *SrHtrI*.<sup>19,20</sup> *SrSRI* is the first discovered and characterized sensory rhodopsin homologue from bacteria. Interestingly, *SrSRI* showed remarkable stability under various conditions, compared to *HsSRI*, which enabled studies which could provide new insight into the Cl<sup>-</sup> binding,<sup>21</sup> a phenomenon also conserved in SRI from *Halorubra vallismortis*.<sup>22</sup> However, it should be noted that the function of *SrSRI* is still unknown, although the secondary sequence, photochemical properties and structural changes of *SrSRI* are very similar to those of the positive phototaxis receptor *HsSRI*.<sup>4,19</sup> In this study, we performed a range of experiments, such as studies using FTIR or UV spectroscopy or testing the reactivity with water-soluble reagents, to obtain better insight into the structure and structural changes of *SrSRI*. The obtained results were compared with those of *NpSRII*.

## MATERIALS AND METHODS

**Sample Preparations.** The wild-type *SrSRI*, *SrSRI-SrHtrI128*, wild-type *NpSRII*, N105D mutant of *NpSRII*, and *HvSRI* expression plasmids were constructed as previously described.<sup>19,20,22–24</sup> The *SrSRI* mutant genes (D2E, D28E, D33E, D35E, D54E, D72E, D102E, D185E, and D197E) and the D105Q SRII mutant gene were constructed by PCR using the QuikChange site-directed mutagenesis method (Stratagene, La Jolla, CA) as described previously.<sup>25</sup> The *Escherichia coli* DH5α strain was used as a host for DNA manipulation. All constructed plasmids were analyzed using an automated sequencer to confirm the expected nucleotide sequences. The preparation of crude membranes and purification of proteins were performed using essentially the same method as described previously.<sup>20</sup> In short, proteins with a six-histidine tag at the C-terminus were expressed in *E. coli* BL21 (DE3) cells as a recombinant protein, solubilized by DDM and purified with a Ni<sup>2+</sup> affinity column. Where necessary, the samples were further purified with an anion exchange column. The samples were concentrated and exchanged using an Amicon Ultra filter (Millipore, Bedford, MA).

**FTIR Spectroscopy.** FTIR spectroscopy was performed with 2 cm<sup>-1</sup> resolution at 260 K, as described previously.<sup>26</sup> The purified proteins were reconstituted into PG liposomes (*SrSRI*:PG molar ratio of 1:50), from which DDM was removed with Bio-Beads (SM-2, Bio-Rad). The PG-reconstituted samples were washed with a 2 mM phosphate buffer (pH 7.0). A droplet of about 40–80 μL of each sample, with a concentration of about 0.5 mg/mL, was dried under vacuum on a BaF<sub>2</sub> window with a diameter of 18 mm, resulting in a homogeneous circular film of a diameter of about 8 mm. This film was hydrated with a trace of H<sub>2</sub>O or D<sub>2</sub>O and sealed and inserted into a Bio-Rad FTS-7000

spectrometer which was equipped with an Oxford Optistat-DN cryostat. To convert *SrSRI* to *SrSRI<sub>M</sub>*, the sample was irradiated for 2 min with light of  $\lambda > 500$  nm through a glass filter (AGC Techno Glass Y-52, Japan) from a 1 kW halogen–tungsten lamp, after which a subsequent 1 min illumination with UV light changed *SrSRI<sub>M</sub>* back to *SrSRI*.<sup>26</sup> The difference spectrum was calculated from the spectra constructed of 128 interferograms before and after the illumination. To increase the quality of the spectra, 24 difference spectra of *SrSRI<sub>M</sub>* minus *SrSRI* were averaged. All spectra were normalized with respect to the C–C or C=C stretching vibration of the retinal chromophore.

**UV-vis Spectroscopy and Time-Resolved Flash Photolysis.** UV-vis spectra were recorded using a UV2450 spectrophotometer with an ISR2200 integrating sphere (Shimazu, Kyoto, Japan). For the reactivity measurements of *SrSRI* with hydroxylamine or azide, samples of a concentration of 1.5 μM were resuspended in the buffers containing 50 mM Tris-HCl (pH 7.0), 1 M NaCl, and 0.1% DDM supplemented with 50 mM hydroxylamine or 0–500 mM azide, respectively. For measuring the reactivity of *HvSRI* with azide, the purified samples were resuspended in a buffer containing 50 mM Tris-HCl (pH 8.5), 1 M NaCl, and 0.1% DDM. High-performance liquid chromatography (HPLC) analysis was performed to obtain information about the composition of the retinal conformation, as described previously.<sup>19</sup> The photocycle kinetics were measured using a conventional flash-photolysis apparatus, following a standard procedure essentially as described previously.<sup>21</sup> Although a phototransient signal could be acquired from a single flash, several kinetic traces were averaged to improve the S/N ratio. The pulse illumination was provided every 25 s with a Xe-flash lamp through a cutoff filter (Y52,  $\lambda > 500$  nm). Bleaching was monitored using the absorbance at 500 nm for *NpSRII* and at 555 nm for *SrSRI*, respectively. The purified sample was exchanged using an Amicon Ultra filter (Millipore, Bedford, MA) against a buffer containing 1 M NaCl (or 333 mM Na<sub>2</sub>SO<sub>4</sub>), 50 mM Tris-Cl (or Tris-SO<sub>4</sub>), and 0.1% DDM, and flash induced absorption changes were acquired at 5 ms intervals. The temperature was kept constant at 298 K.

## RESULTS

**Deprotonation of a Carboxylate in *SrSRI* upon Formation of an Active M-Intermediate.** In 2008, we performed a study using Fourier transform infrared (FTIR) spectroscopy to investigate the structure and the structural changes of *SrSRI* upon formation of the active M-intermediate.<sup>26</sup> In this study, the *SrSRI<sub>M</sub>* minus *SrSRI* difference spectrum exhibited a negative band at 1742 cm<sup>-1</sup> in H<sub>2</sub>O, shifting to 1734 cm<sup>-1</sup> in D<sub>2</sub>O (Figure 1A), suggesting that the band originates from a carboxylate, while a corresponding band in the spectrum of *NpSRII* has not been detected<sup>27</sup> (Figure 1A). The positive bands, which occur in the spectra of both proteins [for *SrSRI* at 1753 cm<sup>-1</sup> in H<sub>2</sub>O, which shifts to 1742 cm<sup>-1</sup> in D<sub>2</sub>O (Figure 1A),<sup>26</sup> and for *NpSRII* at 1764 cm<sup>-1</sup> in H<sub>2</sub>O and at 1753 cm<sup>-1</sup> in D<sub>2</sub>O (Figure 1A)<sup>27</sup>], could be assigned to the C=O stretching vibration of the protonated aspartate group (Asp72 for *SrSRI*; Asp75 for *NpSRII*), which acts as a counterion for the protonated Schiff base (Lys201 for *SrSRI*; Lys205 for *NpSRII*). At a pH higher than the pK<sub>a</sub> of the counterion (as in the case of the reported experiments) the Schiff base counterion is deprotonated in the ground state.<sup>19,28</sup> Upon formation of the M-intermediate, a proton is transferred from the Schiff base to the

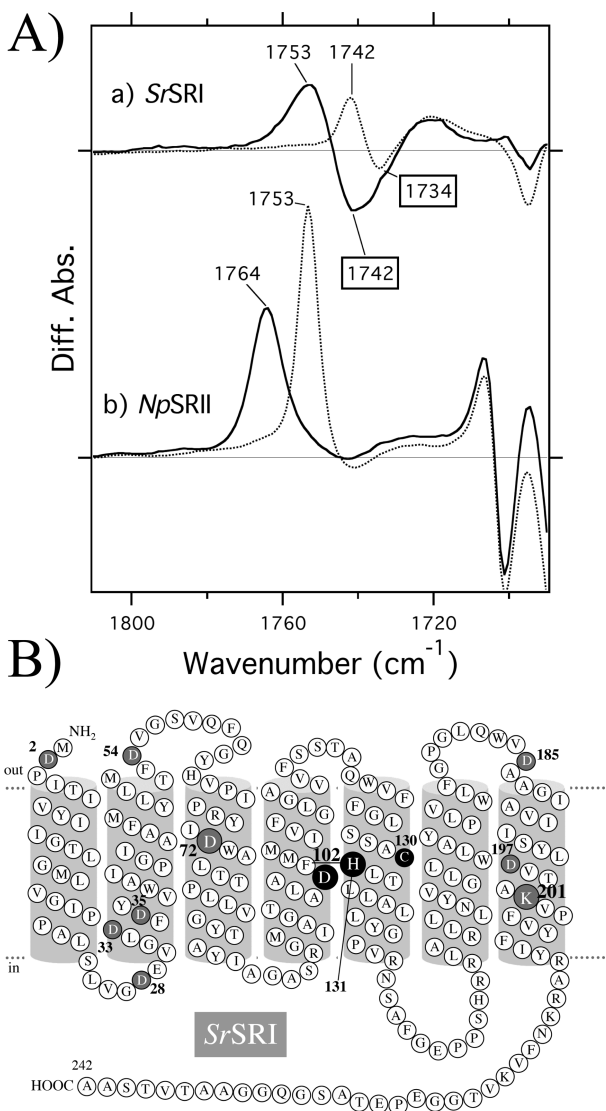


**Figure 1.** (A)  $SrSRI_M$  minus  $SrSRI$  (a) and  $NpSRII_M$  minus  $NpSRII$  (b) difference infrared spectra in the 1810–1690  $\text{cm}^{-1}$  region. Spectra of  $SrSRI$  and  $NpSRII$  are reproduced with some corrections from refs 26 and 27. The samples were hydrated with  $\text{H}_2\text{O}$  (solid line) and  $\text{D}_2\text{O}$  (dotted line). One division of the  $y$ -axis corresponds to 0.0035 absorbance units. (B) Predicted secondary structure of  $SrSRI$ . The primary proton transfer takes place upon formation of the M-intermediate. Then a proton is transferred from the protonated Schiff base (Lys201) to its counterion (Asp72), and a proton may be released from a carboxylic residue.<sup>26</sup> The  $SrSRI$  has nine aspartic acid residues: Asp2, Asp28, Asp33, Asp35, Asp54, Asp72, Asp102, Asp185, and Asp197. His131 is a  $\text{Cl}^-$  binding site in  $SrSRI$ .<sup>21</sup> The sites of attention in this study, Asp102, Cys130, and His131, are colored in black.

counterion, leading to the positive signal which has been observed. The same has been observed in the case of the  $HsSRI$  at alkaline pH, in which the counterion is deprotonated.<sup>29,30</sup> Interestingly, similar to the negative band at 1742  $\text{cm}^{-1}$  which is observed in the spectrum of  $SrSRI$  (Figure 1A), a negative band is also observed in the spectrum of  $HsSRI$  under alkaline conditions at 1734  $\text{cm}^{-1}$ , and this band shifts to 1722  $\text{cm}^{-1}$  in  $\text{D}_2\text{O}$ .<sup>29,30</sup> In both cases the corresponding positive bands are missing. These results indicate that a carboxylate is deprotonated upon formation of the M-intermediate. The frequencies of the negative

bands are typical for aspartates (rather than glutamates). The origin of the negative band in  $HsSRI$  has been discussed before,<sup>29,31,32</sup> and the authors have suggested that this band might arise due to a protonation change (or perturbation) of either Asp201 (homologue of Asp197 in  $SrSRI$ ) or Asp106 (homologue of Asp102 in  $SrSRI$ ).

As can be seen in Figure 1B, in the amino acid sequence of  $SrSRI$ , 9 asparates can be found. To identify the residue causing the negative band, we constructed  $SrSRI$  point mutants, each containing a replacement of one of the nine aspartates (D2E, D28E, D33E, D35E, D54E, D72E, D102E, D185E, and D197E). However, the low stability of D72E, especially in detergent micelles, and the poor expression of D197E in *E. coli* cells, did not allow the measurement of the IR spectrum to a satisfactory quality. Both Asp72 and Asp197 are well conserved among microbial rhodopsins and are thought to be involved in the pentagonal cluster structure around the Schiff base, which is essential for the function of proton pumping rhodopsins.<sup>33</sup> Presumably, the mutations induced structural changes, leading to its decreased stability. In contrast, the other seven mutants (D2E, D28E, D33E, D35E, D54E, D102E, and D185E) were well expressed as recombinant proteins, which have predominantly all-trans-retinal (>90%) as a chromophore, similar to wild-type  $SrSRI$  (>95%),<sup>21</sup> shown by using HPLC analysis.

Figure 2 shows the M minus initial state difference FTIR spectra of wild-type  $SrSRI$  (a) and the D2E (b), D28E (c), D33E (d), D35E (e), D54E (f), D102E (g), and D183E (h) mutants in the 1800–950  $\text{cm}^{-1}$  region obtained at pH 7 and at 260 K. For wild-type  $SrSRI$  (a), the bands at 1526 (−)/1561 (+)  $\text{cm}^{-1}$  can be attributed to the ethylenic C=C stretching vibrations of the retinal chromophore.<sup>26</sup> The shift to higher frequencies corresponds to a spectral blue shift upon formation of the M-intermediate, while the negative bands at 1250, 1199, and 1164  $\text{cm}^{-1}$  can be assigned to the C–C stretching vibrations of the retinal chromophore.<sup>26</sup> The reduced intensity of the corresponding positive bands is caused by the deprotonation of the Schiff base in the M state. Furthermore, the bands at 1666 (+)/1654 (−)  $\text{cm}^{-1}$  can be attributed to the amide-I vibration of the  $\alpha$ -helix. As shown in Figure 2, the spectra of all mutants show almost identical positive and negative peaks in this region, indicating the formation of the M-intermediate in all mutants and that the mutations have no significant effect on the structure and structural changes of  $SrSRI$ . Only in the case of the D102E mutant, a negative band of a C=C stretching vibration appeared at 1529  $\text{cm}^{-1}$ , which is significantly different from all the other spectra. The differences induced by this mutant will be discussed below.

In Figure 3 the spectral changes in the 1790–1690  $\text{cm}^{-1}$  region are shown. This region is typical for the C=O stretching vibrations of protonated carboxylate groups. As can be seen, bands at 1753 (+) and 1742 (−)  $\text{cm}^{-1}$  are observed in the spectrum of wild-type  $SrSRI$  as well as in the spectra of the D2E (b), D28E (c), D33E (d), D35E (e), D54E (f), and D185E (h) mutants, with almost no shift in frequency. The positive band can be tentatively assigned to Asp72, as already mentioned. This band also appears at a similar frequency in the spectrum of the D102E mutant (1753  $\text{cm}^{-1}$  in  $\text{H}_2\text{O}$ ) and shifts to 1749  $\text{cm}^{-1}$  in  $\text{D}_2\text{O}$ , similar to the wild-type (Figure 1A), while the negative band was shifted by 28 to 1714  $\text{cm}^{-1}$ , compared to that of the wild-type. This newly appeared negative band shifts to 1710  $\text{cm}^{-1}$  in  $\text{D}_2\text{O}$ , indicating that the band in D102E can be assigned to the C=O stretching vibration of the introduced Glu

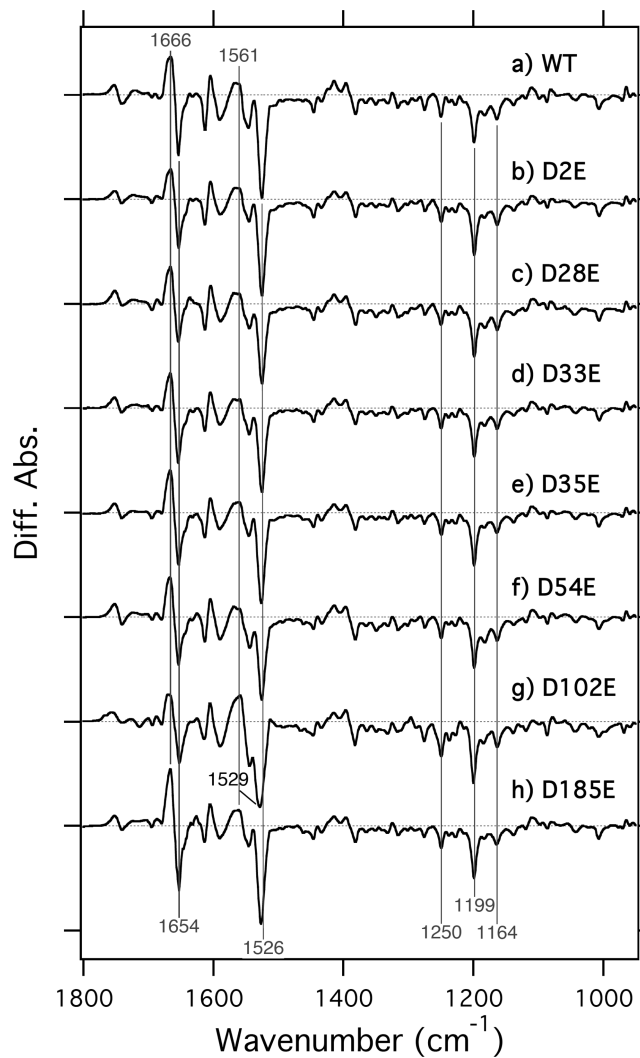


**Figure 2.**  $SrSRI_M$  minus  $SrSRI$  difference infrared spectra for the wild-type (a) and the D2E (b), D28E (c), D33E (d), D35E (e), D54E (f), D102E (g), and D185E (h) mutants measured at 260 K at pH 7.0 in the 1800–950 cm<sup>-1</sup> region. These spectra were normalized with respect to the C=C stretching vibration of the retinal chromophore. The spectrum for the wild-type (a) is reproduced with some corrections from ref 26. The spectra of the D2E (b), D28E (c), D33E (d), D35E (e), D54E (f), D102E (g), and D185E (h) mutants were multiplied by 3.10, 4.90, 1.85, 2.25, 2.18, 1.25, and 1.05 for comparison, respectively. The samples were hydrated with H<sub>2</sub>O. One division of the y-axis corresponds to 0.008 absorbance units.

residue. On the basis of these results, the 1742 cm<sup>-1</sup> band of wild-type  $SrSRI$  can be assigned to the C=O stretching vibration of the protonated Asp102. Interestingly, no frequency shift was induced by the D to E mutation in the region typical for the COO<sup>-</sup> stretching vibrations, around 1400 cm<sup>-1</sup> (Figure 2), because of the insensitivity of the COO<sup>-</sup> group to the induced changes.

**Effects on the S–H Stretching Vibration of Cys130 in  $SrSRI$ .** Frequencies of the cysteine S–H stretches are well isolated from other vibrations occurring in a protein.<sup>34</sup> This is advantageous when analyzing the environmental conditions. In fact, these vibrations could be used for the analysis of engineered BR<sup>35</sup> and SRII,<sup>36</sup> where an alteration in the environment of specific amino acids was monitored by introducing a cysteine

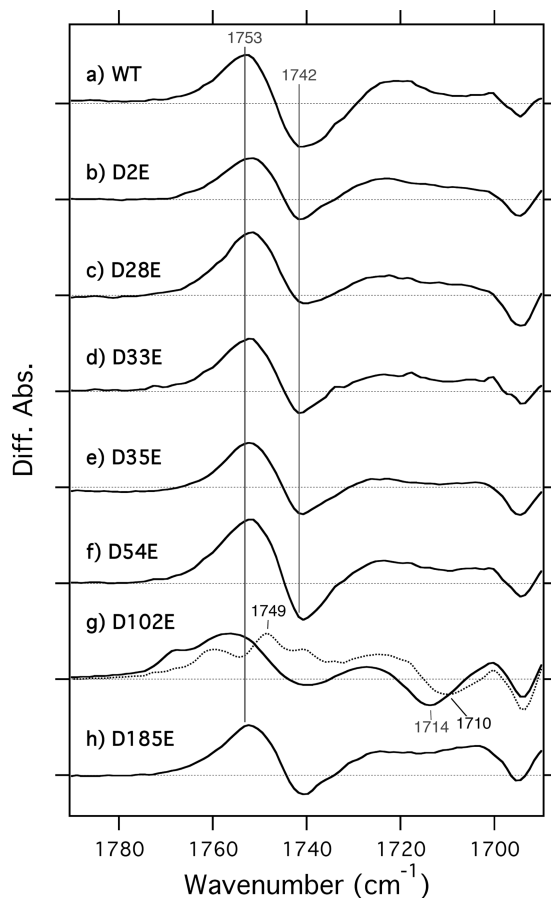


**Figure 3.**  $SrSRI_M$  minus  $SrSRI$  difference infrared spectra for the wild-type (a) and the D2E (b), D28E (c), D33E (d), D35E (e), D54E (f), D102E (g), and D185E (h) mutants measured at 260 K at pH 7.0 in the 1790–1690 cm<sup>-1</sup> region. The samples were hydrated with H<sub>2</sub>O (solid line) and D<sub>2</sub>O (dotted line). The spectrum of D102E in D<sub>2</sub>O was corrected by the subtraction of the spectrum obtained in H<sub>2</sub>O (10%), and the subtracted spectrum was multiplied by 1.45 for comparison. One division of the y-axis corresponds to 0.0015 absorbance units.

residue. In the case of  $SrSRI$ , which has only one cysteine residue (Cys130) (Figure 1B) that is conserved in bacterial SRI proteins,<sup>19</sup> the S–H stretching vibration can provide insight into the local environmental conditions. Figure 4 shows the spectral changes in the 2600–2500 cm<sup>-1</sup> region, typical for S–H stretching vibration. No vibrational band is observed in the spectrum of wild-type  $SrSRI$  or in those of the D2E (b), D28E (c), D33E (d), D35E (e), D54E (f), and D185E (h) mutants. In contrast, in the spectrum of the D102E mutant, S–H vibrational bands appeared at 2549 (−)/2561 (+) cm<sup>-1</sup> (g), indicating that the D to E mutation of Asp102 (which is simply an addition of a C–H<sub>2</sub> group) affects locally the structure and structural changes of  $SrSRI$ . The upshift of the S–H stretching vibration of Cys130, upon formation of the M-intermediate, suggests that the hydrogen bond of S–H is strengthened.

**Absorption Maximum and Protein Stability of the D102E Mutant.** In Figure 2g, the C=C stretching band for D102E is shifted to lower frequencies (1529 cm<sup>-1</sup>), compared to the wild-type (1526 cm<sup>-1</sup>) or to the other Asp mutants, suggesting a spectral blue shift in the D102E mutant. To confirm this, we measured its UV–vis absorption spectrum at room temperature. Figure 5a shows the absorption spectra of wild-type  $SrSRI$

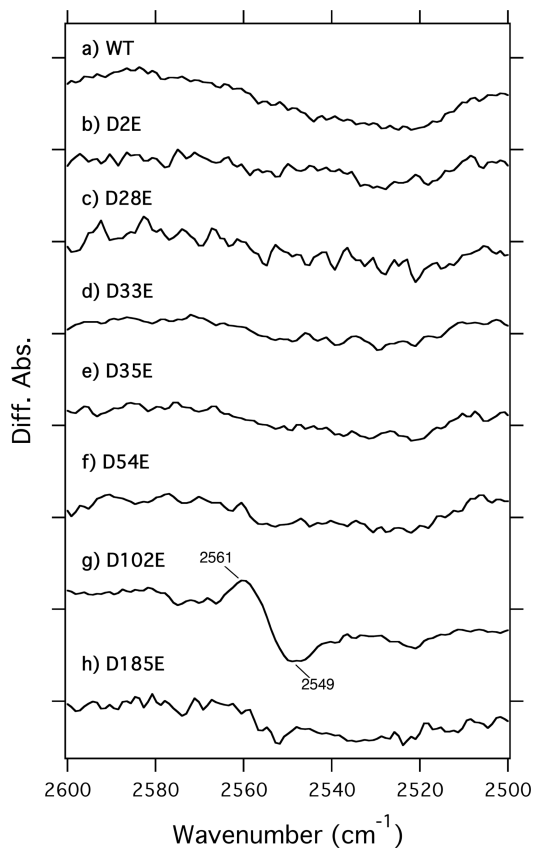


**Figure 4.**  $SrSRI_M$  minus  $SrSRI$  difference infrared spectra for the wild-type (a) and the D2E (b), D28E (c), D33E (d), D35E (e), D54E (f), D102E (g), and D185E (h) mutants measured at 260 K at pH 7.0 in the  $2600\text{--}2500\text{ cm}^{-1}$  region. The samples were hydrated with  $H_2O$ . One division of the y-axis corresponds to 0.0002 absorbance units.

(dotted line) and the D102E mutant (solid line). The  $\lambda_{\max}$  of D102E (539 nm) was greatly shifted to lower wavelengths, compared to that of wild-type  $SrSRI$  (557 nm). Furthermore, it lies close to the  $\lambda_{\max}$  of wild-type  $SrSRI$  in the absence of anions (542 nm).<sup>21</sup> To investigate whether the spectral change was caused by the lack of anion binding to the protein, we measured the dependence of the absorption spectrum, and photocycle kinetics of the D102E mutant, on salt concentration. As shown in Figure 5b, the absorption maximum of the mutant in the absence of  $Cl^-$  was located at 529 nm, i.e., 10 nm spectral blue-shifted ( $\Delta\nu = 350\text{ cm}^{-1}$ ), similar to the shift observed in wild-type  $SrSRI$  (557 nm  $\rightarrow$  542 nm). Furthermore,  $Cl^-$  binding has been shown to affect the photocycle kinetics of  $SrSRI$ .<sup>21</sup> In the case of the D102E mutant, the time dependence of the change in absorbance at 380 nm for the M-state and at 540 nm for the original state are shown in Figure 5c. The data could be well fitted with a single-exponential decay equation, and the rate constant ( $K_t$ ) was estimated to be  $1.0\text{ s}^{-1}$  in 1 M NaCl. In contrast, the rate constant in the absence of  $Cl^-$  was 3.9-fold larger ( $K_t = 3.9\text{ s}^{-1}$ ), compared to that in a 1 M NaCl solution, similar to the changes observed in the wild-type.<sup>21</sup> Thus, the  $\lambda_{\max}$  must be affected by the addition of the C-H<sub>2</sub> group by the D to E mutation at position 102 (D102E). The residue Asp102 is completely conserved in the family of SRI proteins,<sup>19</sup> while the corresponding amino acid is replaced with Asn105 in SRII.<sup>24</sup> In the case of  $NpSRII$ , the  $\lambda_{\max}$  of the WT was almost identical to those of the N105Q and N105D

mutants (Figure 5d), supporting the local structural difference between SRI and SRII around the residue.

Figure 6 shows flash-induced bleaches of  $SrSRI$ ,  $NpSRII$ , and their mutants. The normalized numbers of unbleached pigments, estimated by the amplitude of flash photolysis (at 555 nm for wild-type  $SrSRI$ , 540 nm for D102E, and 500 nm for wild-type  $NpSRII$  and N105Q), are plotted against the number of flashes of light ( $\lambda > 460\text{ nm}$ ). The data could be fitted with a single-exponential equation. As shown in Figure 6a, the bleaching rate of wild-type  $SrSRI$  is lower in the presence of  $Cl^-$  (open circles) than in the  $Cl^-$ -free case (closed circles), whereas no significant change was caused by the change in  $Cl^-$  concentration in the case of SRII (c). The effect of the absence of  $Cl^-$  is greatly enhanced by the D102E mutation (b), whereas no significant effect was observed in the N105Q mutant of SRII (d). It should be noted that even in the presence of  $Cl^-$   $SrSRI$  is slowly bleached under light for both the wild-type and the D102E mutant (open circles in panel A), while in the dark almost no bleaching was observed,<sup>19</sup> indicating that the photointermediate(s) is more unstable than the unphotolyzed state. It is likely that it is the M-intermediate which is the unstable photointermediate because of its long lifetime ( $\sim$ seconds) (see Figure 5c). Thus, Asp102 seems to be involved in the maintenance of the proper structure, in both the unphotolyzed and photolyzed states, in contrast to the corresponding residue in  $NpSRII$ .

**Reactivity of  $SrSRI$  with the Water-Soluble Reagents, Hydroxylamine and Azide, in the Presence and Absence of  $SrHtrI$ .** To investigate the difference between SRI and SRII around the Schiff base of the retinal chromophore, we measured the reactivity of  $SrSRI$  with water-soluble reagents, and compared the results with those of SRII. Although SRII is a membrane protein, hydroxylamine and azide have been shown to be able to react with SRII: (1) hydroxylamine attacks the Schiff base to bleach the pigment,<sup>17</sup> and (2) azide accelerates selectively the decay of the M-intermediate.<sup>17</sup> The increase in reactivity of these reagents is mainly caused by the increase in the accessibility of the comparably hydrophilic Schiff base via the hydrophobic moiety inside the protein. Therefore, the reactivity is a good indicator of the environment and the environmental change in the region around the Schiff base.

Figure 7 shows the absorption spectra of  $SrSRI$  alone (a) and of the  $SrSRI$ - $SrHtrI128$  complex (b) at several times after the addition of hydroxylamine.  $SrHtrI128$  is the truncated  $SrHtrI$ , expressed from position 1 to 128, which is sufficient for the interaction with  $SrSRI$ .<sup>20</sup> As can be seen, decreases in the absorbance at 557 nm for  $SrSRI$  and at 543 nm for  $SrSRI$ - $SrHtrI128$ , and concomitant increases in the absorbance at 364 nm in both cases, the presence and absence of  $SrHtrI$ , were observed, while no spectral change could be observed in the absence of light or hydroxylamine. The changes in the peaks are proportional to each other, with an isosbestic point found at around 400 nm (a and b), implying that hydroxylamine can attack the Schiff base of  $SrSRI$  in both the presence and absence of  $SrHtrI$ . In Figure 7c, the absorbance of  $SrSRI$  (open circles) and the  $SrSRI$ - $SrHtrI128$  complex (closed circles) is plotted against the time in the absence of light. The bleaching rates of  $SrSRI$  and the  $SrSRI$ - $SrHtrI128$  complex were calculated to be  $0.013$  and  $0.028\text{ min}^{-1}$ , respectively. This indicates that the reaction of  $SrSRI$  with hydroxylamine is 2.2-fold slower compared to that of the complex with  $SrHtrI$ . A similar trend can be observed in the case of  $NpSRII$  in the dark, in which the removal of  $NpHtrII$  decelerates the bleaching rate 1.4-fold,<sup>17</sup> suggesting

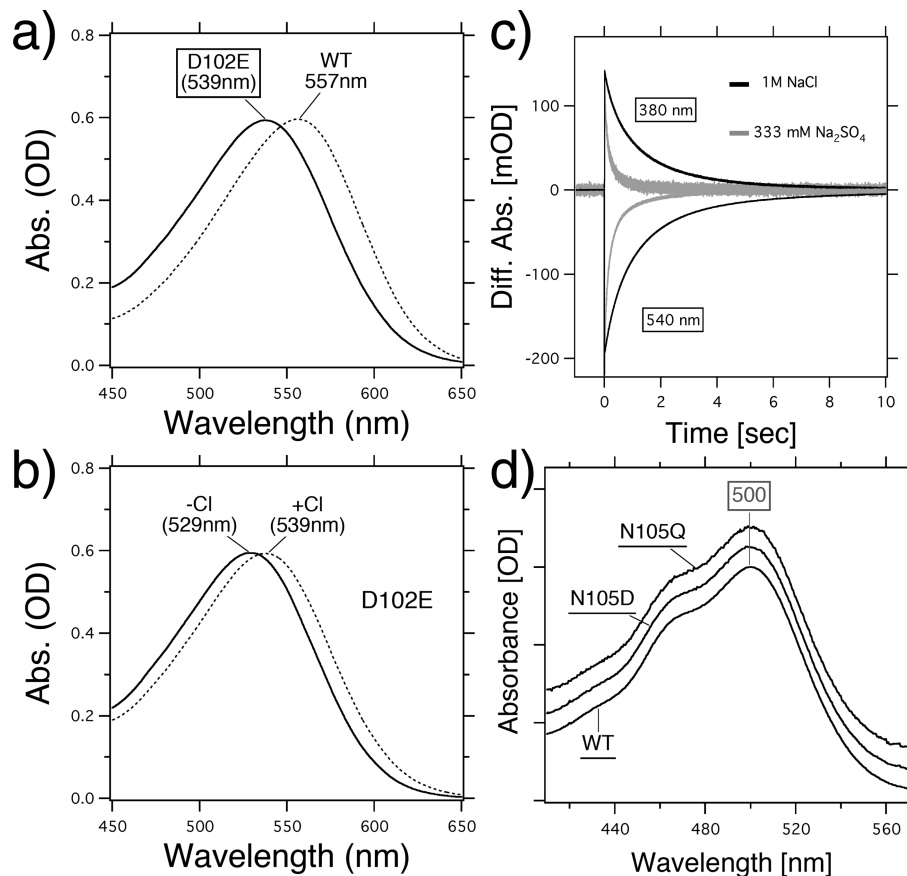


**Figure 5.** (a) Absorption spectra of DDM-solubilized SrSRI for the wild-type (dotted line) and the D102E mutant (solid line) over a spectral range from 450 to 650 nm. The samples were suspended in a buffer containing 50 mM Tris-H<sub>2</sub>SO<sub>4</sub> (pH 7.0), 0.1% DDM, and 1 M NaCl. (b) Absorption spectra of the DDM-solubilized D102E mutant in a buffer containing 50 mM Tris-H<sub>2</sub>SO<sub>4</sub> (pH 7.0) and 0.1% DDM with 1 M NaCl (dotted line) and without NaCl (solid line) over a spectral range from 450 to 650 nm. The ionic strength was kept constant using 333 mM Na<sub>2</sub>SO<sub>4</sub>. (c) Flash-induced kinetic data of the D102E mutant in a buffer containing 50 mM Tris-H<sub>2</sub>SO<sub>4</sub> (pH 7.0) and 0.1% DDM with 1 M NaCl (black) and 333 mM Na<sub>2</sub>SO<sub>4</sub> (gray). The temperature was kept constant at 25 °C. The M-intermediate and initial state of SrSRI were monitored at 380 and 540 nm, respectively. (d) Absorption spectra of DDM-solubilized *Np*SRII for the wild-type and the N105D and N105Q mutants over a spectral range from 410 to 570 nm. The samples were suspended in a buffer containing 50 mM Tris-H<sub>2</sub>SO<sub>4</sub> (pH 7.0), 0.1% DDM, and 1 M NaCl. One division of the y-axis corresponds to 0.4 absorbance units. The spectra of N105D and N105Q were shifted by 0.1 and 0.2, respectively, for comparison. The protein concentration was adjusted to 15 μM.

that the transducer protein-induced structural changes between SRI and SRII are similar. However, one should note that these bleaching rates are very small, which indicate the closed conformations of the unphotolyzed states in both SrSRI and *Np*SRII in the presence and absence of their cognate transducer proteins.

The decay of the M-intermediate corresponds to the reprotonation process of the Schiff base. In agreement with this, Takao et al. reported that azide accelerates the *Np*SRII<sub>M</sub> decay,<sup>17</sup> implying that azide can provide protons to the deprotonated Schiff base of *Np*SRII<sub>M</sub>, while for SRI the effects of azide have not been reported so far. Figure 8 shows the changes in the absorbance of the M-intermediate of SrSRI (Figure 8a) and the SrSRI–SrHtrI128 complex (Figure 8b) over a range of azide concentrations. Almost no dependence on the azide concentration can be observed for the M-decay of SrSRI, while the M-decay of the SrSRI–SrHtrI complex is enhanced by over 3 orders of magnitude in an azide-dependent manner (Figure 8c). The change in the decay constant could be fitted with a Michaelis–Menten-like equation with respect to the added azide concentration. Interestingly, no effect of azide on the M-decay was also observed for the SRI of another species, the archaeon

*Haloarcula vallismortis* (*Hv*SRI) (Figure 8c). In the case of *Np*SRII, the acceleration of the M-decay was about 4.6-fold slower in the case of the *Np*SRII–*Np*HtrII complex compared to *Np*SRII.<sup>17</sup> Thus, the transducer binding to SrSRI has the opposite effect on the reactivity with azide compared to *Np*SRII, indicating (1) structural differences in the M state between SrSRI and *Np*SRII and between the SrSRI–SrHtrI and the *Np*SRII–*Np*HtrII complexes and (2) differences in the structural changes induced by the complex formation with the cognate Htr.

## ■ DISCUSSION

**Structure and Structural Changes around the β-Ionone Ring of the Retinal Chromophore in SrSRI.** In this study, we investigated the structure and structural changes of SrSRI, summarized in Figure 9, by using a range of techniques and compared the obtained results to those of SRII. We demonstrated that Asp102 in SrSRI is deprotonated upon formation of the active M-intermediate (Figure 3). A similar phenomenon has been reported for BR, in which the M-formation is accompanied by the release of a proton from a protonated water cluster

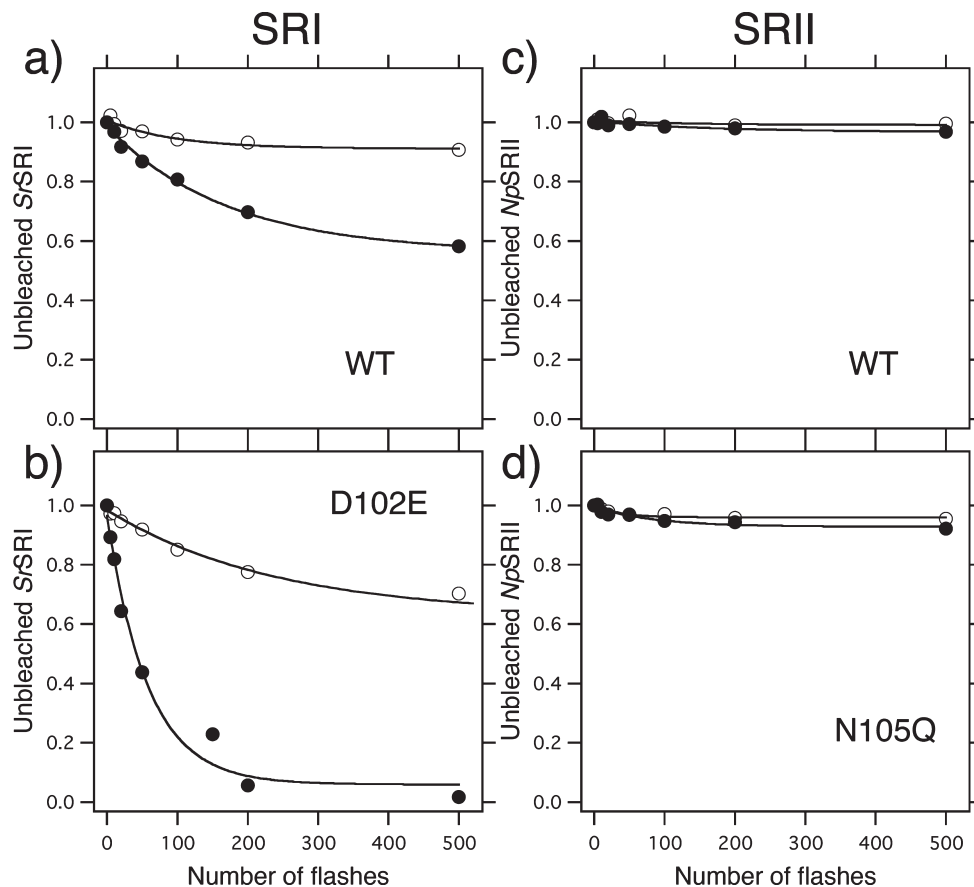


**Figure 6.** Flash-induced bleaches for SrSRI (a), the D102E mutant of SrSRI (b), NpSRII (c), and the N105Q mutant of NpSRII (d). The ordinate represents the normalized numbers of unbleached (alive) pigments estimated by the amplitude of flash photolysis (at 555 nm for WT SrSRI, 540 nm for D102E, and 500 nm for WT NpSRII and the N105Q mutant), and the abscissa represents the number of flashes. The samples were suspended in a buffer containing 50 mM Tris-H<sub>2</sub>SO<sub>4</sub> (pH 7.0) and 0.1% DDM with 1 M NaCl (open circles) and without NaCl (closed circles). The ionic strength was kept constant using 333 mM Na<sub>2</sub>SO<sub>4</sub>. The temperature was kept constant at 25 °C. The protein concentration was adjusted to 15 μM.

(not from a carboxylic acid, as in the case of SrSRI) around the Schiff base of the retinal chromophore to the periplasm.<sup>37,38</sup> It should be noted that a change in the state of Asp115 (the homologous residue for Asp102 in BR) was first detected in the photocycle of BR in 1988 using site-directed mutagenesis and FTIR spectroscopy.<sup>39</sup> This is important to note since it establishes that this residue is involved in proton pumping. However, the presence of a positive band appearing as early as in the K-intermediate led to the conclusion that this group does not deprotonate, but rather undergoes a change in hydrogen bonding. What are the proton acceptor and donor in SrSRI? In microbial rhodopsin molecules, the region around the β-ionone ring is characterized by its high hydrophobicity, in which no suitable candidate for both the acceptor and donor can be found. Therefore, it could be assumed that, in the case of SrSRI, the proton of Asp102 might be released to the cytoplasm or periplasm upon formation of the M-intermediate and from there directly taken up upon recovery to the original state (Figure 9). However, the fate of the proton has to be left undecided, until direct evidence has been obtained. Interestingly, a similar negative band at 1735 cm<sup>-1</sup> has been observed in the spectrum of HsSRI,<sup>29,30</sup> indicating that the deprotonation of Asp102 in SrSRI may also be common to other SRI proteins. Although the role of Asp102 on the proton pumping activity of SrSRI is interesting, it is hard to measure the activity of both the wild-type and the

mutants because of their low pumping activity. Highly sensitive electrodes, such as SnO<sub>2</sub>,<sup>23</sup> will likely be needed.

Furthermore, the addition of a C–H<sub>2</sub> group in Asp102 of SrSRI (i.e., the D102E mutant) induces a structural perturbation of Cys130 (Figure 4), a large visible spectral shift (Figure 5), and a decrease in the protein stability, especially in the absence of Cl<sup>-</sup> (Figure 6). The β-ionone ring of the retinal chromophore is assumed to be sandwiched between Asp102 and Cys130 (Figure 9). Cys130 is conserved among eubacterial SRI proteins<sup>19</sup> and is located prior to His131, a conserved residue among SRI proteins. We have previously concluded that this His131 residue is involved in the Cl<sup>-</sup> binding in SrSRI because the H131F and H131A mutants did not show a Cl<sup>-</sup>-induced spectral shift or acceleration of the M-decay.<sup>21</sup> The phenomenon of Cl<sup>-</sup> binding has also been observed in other SRI, such as HvSRI.<sup>22</sup> It is likely that the binding of the chloride ion to SRI is important for its function in the phototaxis response by optimizing its absorption maximum and maintaining a slow photocycle. His131 of SrSRI is located close to the β-ionone ring, as is Asp102 (Figures 1B and 9). Thus, the residues responsible for changes in the structure, and structural changes in SrSRI (Asp102, Cys130, and His131), are concentrated around the β-ionone ring of the retinal chromophore (Figure 9). In contrast to this, similar mutations in NpSRII (N105Q and N105D) did not affect the absorption maximum or protein stability (Figures 5 and 6),

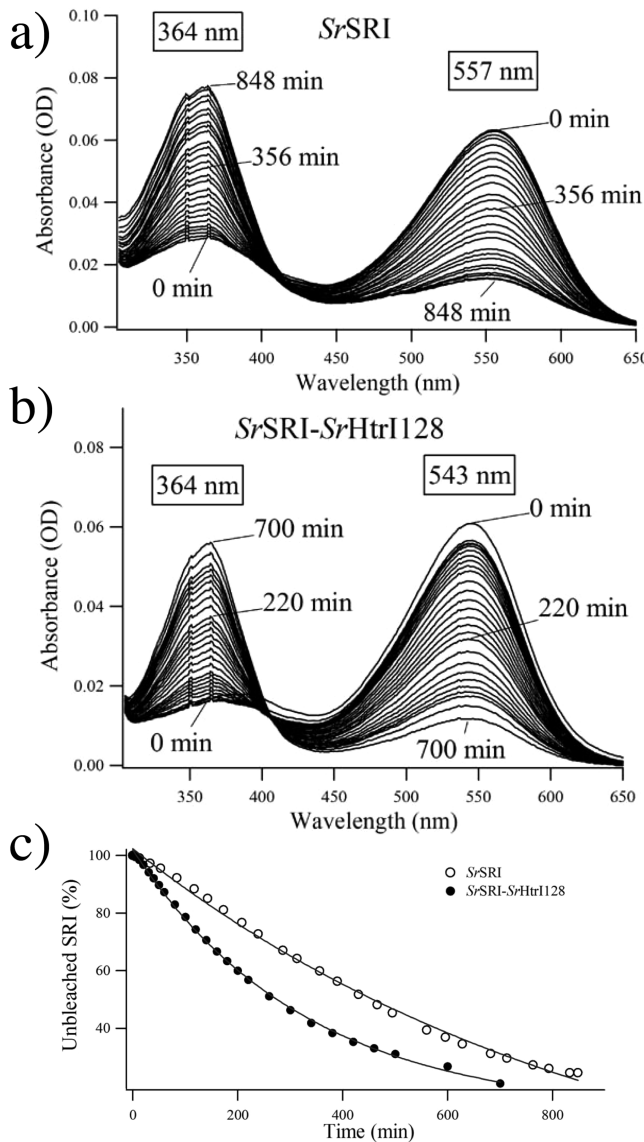


**Figure 7.** Reactivity of *SrSRI* (a) and the *SrSRI*–*SrHtrI128* fusion complex (b) with hydroxylamine in the dark. The spectra were recorded at several times after the addition of hydroxylamine (50 mM). Samples of 1.5  $\mu$ M were suspended in a buffer containing 50 mM Tris-HCl (pH 7.0), 1 M NaCl, and 0.1% DDM. The temperature was kept constant at 25 °C. (c) Bleaching kinetics of *SrSRI* (open circles) and the *SrSRI*–*SrHtrI128* fusion complex (closed circles) in the dark. The data were fitted with a single-exponential equation to estimate the rate constants.

indicating that the structure, and structural changes, around the  $\beta$ -ionone ring between *SrSRI* and *NpSRII* are considerably different. In the case of SRII, the following structural changes have been proposed to be essential for its function:<sup>3,4</sup> (i) the *trans*–*cis* photoisomerization of the retinal chromophore, (ii) the steric hindrance between the C14–H group of the retinal (around the Schiff base) and Thr204,<sup>40</sup> and (iii) the alteration in the hydrogen bonding between Thr204 and Tyr174,<sup>25</sup> which are located at the Schiff base region in SRII near the HtrII binding surface. Interestingly, only the mutants T204A and Y174F were reported to impair the phototaxis response.<sup>41</sup>

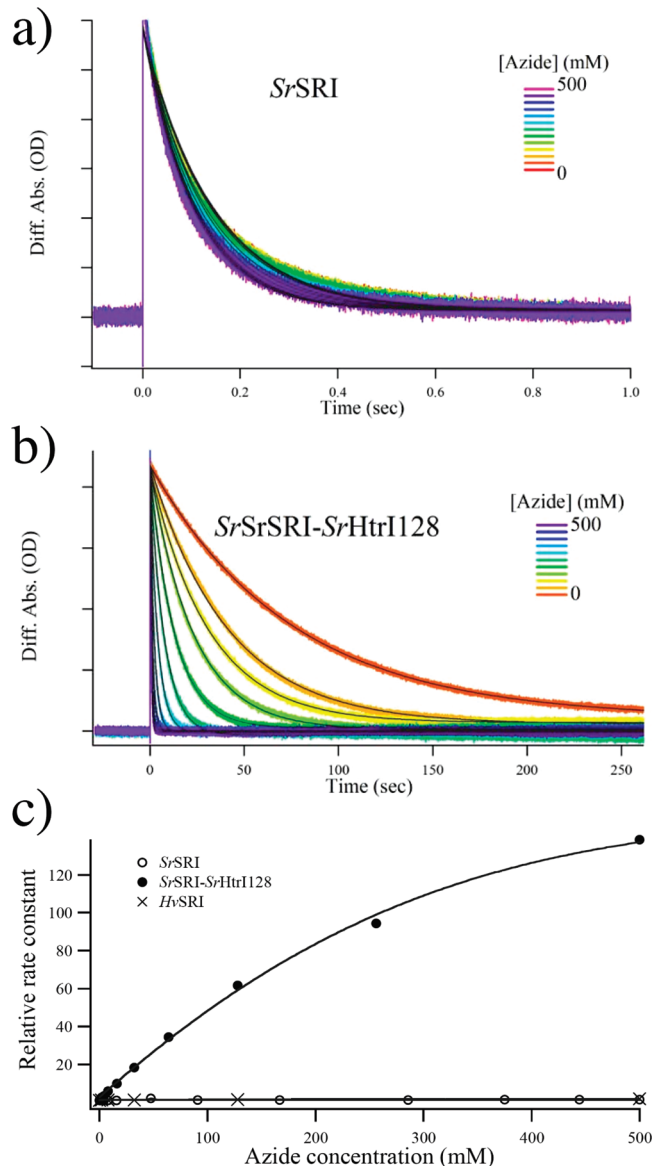


**Figure 8.** Effects of azide on the M-decay of *SrSRI* (a) and the *SrSRI*–*SrHtrI128* fusion complex (b). The data were fitted with a single-exponential equation to estimate the rate constants. Samples of 5  $\mu$ M were suspended in a buffer containing 50 mM Tris-HCl (pH 7.0), 1 M NaCl, and 0.1% DDM at various concentrations (0–500 mM) of azide. The temperature was kept constant at 30 °C. (c) Relative M-decay rates (rate(0 mM) = 1) are plotted against the concentration of azide. Open circles and closed circles represent *SrSRI* and the *SrSRI*–*SrHtrI128* complex, respectively. The purified *HvSRI* (cross) was resuspended in an alkaline buffer, containing 50 mM Tris-HCl (pH 8.5), 1 M NaCl, and 0.1% DDM, in which the counterion of the Schiff base is deprotonated.

**Structure and Structural Changes around the Schiff Base Region in *SrSRI*.** To investigate the structure and structural changes around the Schiff base of *SrSRI*, we measured the reactivity with the water-soluble reagents, hydroxylamine and azide (Figures 7 and 8). As for the case of *NpSRII*, the reactivity of *SrSRI* with hydroxylamine is increased upon formation of the complex with its Htr, which has been interpreted as a cytoplasmic opening, induced by the transducer protein in the unphotolyzed state. This can lead to an increase in the hydrophilicity around the

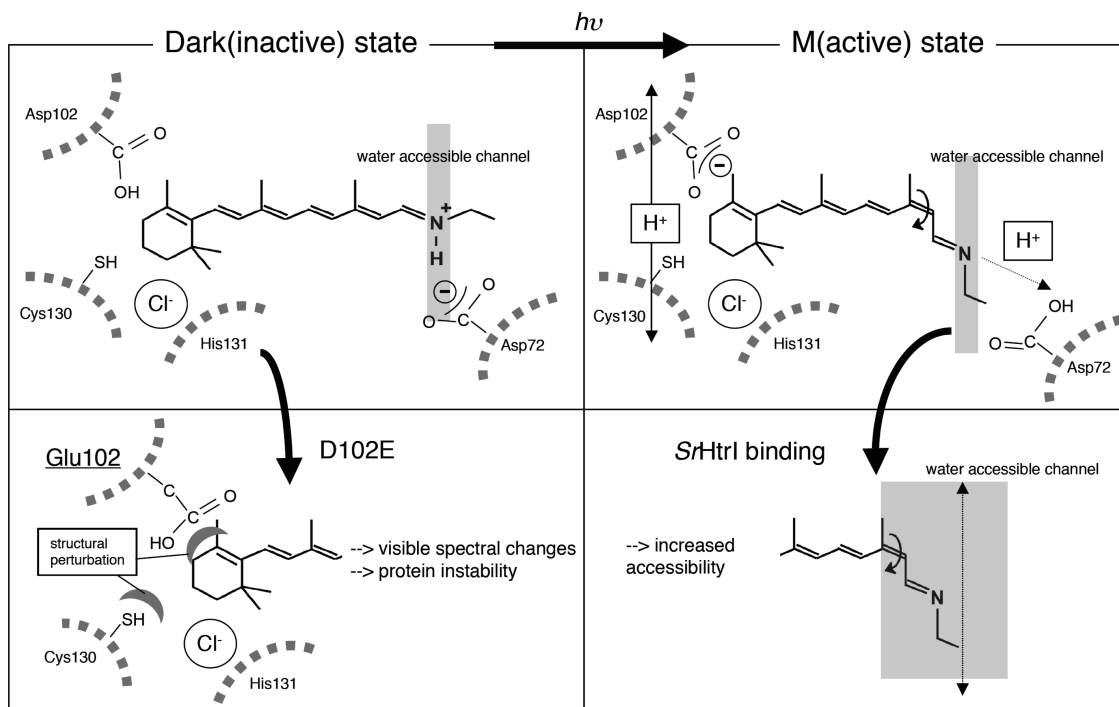


**Figure 9.** Schematic diagram of the structure and structural changes of SrSRI in both the unphotolyzed and photoactivated states. An  $\text{H}^+$  may be released from Asp102 to the cytoplasm or periplasm upon formation of an active M-intermediate. However, the fate of the proton has to be left undecided, until direct evidence has been obtained. The  $\text{H}^+$  of the Schiff base is transferred to the counterion Asp72 in the M-intermediate. D to E mutation of Asp102 (which is simply an addition of a  $\text{C}-\text{H}_2$  group) affects locally the structure and structural changes of SrSRI. The binding SrHtrI to SrSRI leads to an increase in hydrophilicity around the Schiff base in the M-intermediate of SrSRI.

Schiff base. Furthermore, studies of the reactivity with azide gave insight into the changes in the active M-intermediate. In the case of *NpSRII*, the *NpHtrII*-free *NpSRII* protein has a 4.6-fold larger reactivity with azide, compared to that of the complex with *NpHtrII*.<sup>17</sup> It has been reported that a proton uptake occurs during the  $\text{SRII}_M$  decay and that an electrogenic proton transport from the cytoplasmic to the extracellular space is observed in the case of *NpHtrII*-free *NpSRII*.<sup>23</sup> This has been interpreted as follows: during the presence or decay of the  $\text{SRII}_M$ , a cytoplasmic (CP) channel may open, leading to an increase in the water accessibility of the Schiff base, which results in an increase in reactivity with water-soluble reagents. However, once *NpSRII* associates with *NpHtrII*, the electrogenic proton transport stops, and only a proton circulation occurs.<sup>23</sup> Furthermore, several reports on the structure of BR and its mutants<sup>42,43</sup> reveal movement of the helices during the photocycle. The conformational change is largely located at the cytoplasmic end of helices F and G. These movements open a narrow water-accessible channel in the protein, enabling the transfer of a proton from an aspartate residue to the Schiff base. Similar movements of helices during the photocycle were suggested for *NpSRII* by studies using electron paramagnetic resonance spectroscopy,<sup>15</sup> while the photoinduced outward tilting of helix F (or G) is hampered by *NpHtrII*.<sup>16</sup> Thus, the decrease in the reactivity of *NpSRII* with azide can be interpreted by the closure of the CP channel. In the case of *SrHtrI*-free SrSRI, the reactivity with azide is more than 1000-fold smaller than that in the case of the complex with *SrHtrI*. By drawing an analogy with SRII, an inward tilting of helix F of  $\text{SrSRI}_M-\text{SrHtrI}$  might occur. We demonstrated by using FTIR spectroscopy that the frequency shifts of the amide-I and amide-A vibrations of the  $\alpha$ -helix, upon formation of

the M-intermediate, were opposite between SrSRI and *NpSRII* (a downshift and an upshift were observed, respectively).<sup>26</sup> This indicates that the M formation is accompanied by a weakening of the hydrogen bonds of the  $\alpha$ -helix in SRI, while the hydrogen bonds of the  $\alpha$ -helix in SRII are strengthened. Thus, the change of reactivity with azide can be related to the FTIR results.

Recently, opposite conformations during attractant and repellent signaling of the *HsSRI-HsHtrI* and *NpSRII-NpHtrII* complexes have been reported from changes in the Schiff base connectivity switch (inward/outward).<sup>44,45</sup> This signaling behavior may be well described with the two-state model for receptor signaling, which is most extensively studied in the case of chemoreceptors.<sup>1</sup> In the unphotolyzed state, the SRI-HtrI and SRII-HtrII complexes favor the kinase states ON and OFF, respectively, while in the M-intermediate, they change their preference to the other kinase states. Furthermore, the dynamic properties of the F-helices of the SRI-HtrI and SRII-HtrII complexes in the M-intermediate are consistent with the “frozen dynamic” model of chemoreceptors, in which the kinase inactivating receptor is more dynamic than the kinase activating one.<sup>46</sup>

In conclusion, we obtained new insight into the structural changes around the retinal chromophore in SrSRI upon formation of the active M intermediate. In comparison with previously reported studies on a range of microbial rhodopsin molecules, the experimental results could be correlated with movements of protons and the opening of a water accessible channel in the SrSRI protein. Those movements differ from the ones observed in the negative phototaxis receptor.

## ■ AUTHOR INFORMATION

### Corresponding Author

\*Tel +81-52-789-2993; Fax +81-52-789-3001; e-mail z47867a@cc.nagoya-u.ac.jp.

### Author Contributions

<sup>†</sup>H.I. and L.R. contributed equally to this work.

### Funding Sources

This work was financially supported by grants from the Japanese Ministry of Education, Culture, Sports, Science, and Technology to M.H. (18074003), H.K. (22247024 and 20108014), and Y.S. (20050012 and 22018010).

## ■ ACKNOWLEDGMENT

We thank Dr. Tatsuya Iwata for expert technical assistance in FTIR spectroscopy, and we are also grateful to Daisuke Suzuki and Yukie Kawase for assistance in sample preparation.

## ■ ABBREVIATIONS

DDM, *n*-dodecyl- $\beta$ -D-maltoside; SRI, sensory rhodopsin I; SRII, sensory rhodopsin II; HtrI, halobacterial transducer protein for SRI; HtrII, halobacterial transducer protein for SRII; SRI–HtrI, complex of SRI and HtrI; SrSRI, SRI from *Salinibacter ruber*; SrHtrI, HtrI from *Salinibacter ruber*; SrSRI–SrHtrI128, fusion complex of SrSRI and truncated SrHtrI expressed from position 1 to 128; SrSRI<sub>M</sub>, M-intermediate of SrSRI; PG, L- $\alpha$ -phosphatidyl glycerol.

## ■ REFERENCES

- (1) Falke, J. J., Bass, R. B., Butler, S. L., Chervitz, S. A., and Danielson, M. A. (1997) The two-component signaling pathway of bacterial chemotaxis: a molecular view of signal transduction by receptors, kinases, and adaptation enzymes. *Annu. Rev. Cell Dev. Biol.* 13, 457–512.
- (2) Hoff, W. D., Jung, K. H., and Spudich, J. L. (1997) Molecular mechanism of photosignaling by archaeal sensory rhodopsins. *Annu. Rev. Biophys. Biomol. Struct.* 26, 223–258.
- (3) Klare, J. P., Chizhov, I., and Engelhard, M. (2008) Microbial rhodopsins: scaffolds for ion pumps, channels, and sensors. *Results Probl. Cell Differ.* 45, 73–122.
- (4) Suzuki, D., Irieda, H., Homma, M., Kawagishi, I., and Sudo, Y. (2010) Phototactic and chemotactic signal transduction by transmembrane receptors and transducers in microorganisms. *Sensors* 10, 4010–4039.
- (5) Chen, X., and Spudich, J. L. (2002) Demonstration of 2:2 stoichiometry in the functional SRI-HtrI signaling complex in Halobacterium membranes by gene fusion analysis. *Biochemistry* 41, 3891–3896.
- (6) Gordeliy, V. I., Labahn, J., Moukhamedzianov, R., Efremov, R., Granzin, J., Schlesinger, R., Buldt, G., Savopol, T., Scheidig, A. J., Klare, J. P., and Engelhard, M. (2002) Molecular basis of transmembrane signalling by sensory rhodopsin II-transducer complex. *Nature* 419, 484–487.
- (7) Spudich, J. L., Yang, C. S., Jung, K. H., and Spudich, E. N. (2000) Retinylidene proteins: structures and functions from archaea to humans. *Annu. Rev. Cell Dev. Biol.* 16, 365–392.
- (8) Takahashi, T., Tomioka, H., Kamo, N., and Kobatake, Y. (1985) A photosystem other than PS370 also mediates the negative phototaxis of Halobacterium halobium. *FEMS Microbiol. Lett.* 28, 161–164.
- (9) Lanyi, J. K. (2004) Bacteriorhodopsin. *Annu. Rev. Physiol.* 66, 665–688.
- (10) Essen, L. O. (2002) Halorhodopsin: light-driven ion pumping made simple? *Curr. Opin. Struct. Biol.* 12, 516–522.
- (11) Sudo, Y., Yamabi, M., Iwamoto, M., Shimono, K., and Kamo, N. (2003) Interaction of *Natronobacterium pharaonis* phoborhodopsin (sensory rhodopsin II) with its cognate transducer probed by increase in the thermal stability. *Photochem. Photobiol.* 78, 511–516.
- (12) Sudo, Y., Iwamoto, M., Shimono, K., and Kamo, N. (2002) Tyr-199 and charged residues of *pharaonis* phoborhodopsin are important for the interaction with its transducer. *Biophys. J.* 83, 427–432.
- (13) Sudo, Y., Yamabi, M., Kato, S., Hasegawa, C., Iwamoto, M., Shimono, K., and Kamo, N. (2006) Importance of specific hydrogen bonds of archaeal rhodopsins for the binding to the transducer protein. *J. Mol. Biol.* 357, 1274–1282.
- (14) Sudo, Y., and Spudich, J. L. (2006) Three strategically placed hydrogen-bonding residues convert a proton pump into a sensory receptor. *Proc. Natl. Acad. Sci. U.S.A.* 103, 16129–16134.
- (15) Wegener, A. A., Chizhov, I., Engelhard, M., and Steinhoff, H. J. (2000) Time-resolved detection of transient movement of helix F in spin-labelled *pharaonis* sensory rhodopsin II. *J. Mol. Biol.* 301, 881–891.
- (16) Wegener, A. A., Klare, J. P., Engelhard, M., and Steinhoff, H. J. (2001) Structural insights into the early steps of receptor-transducer signal transfer in archaeal phototaxis. *EMBO J.* 20, 5312–5319.
- (17) Sudo, Y., Iwamoto, M., Shimono, K., and Kamo, N. (2002) Association of *pharaonis* phoborhodopsin with its cognate transducer decreases the photo-dependent reactivity by water-soluble reagents of azide and hydroxylamine. *Biochim. Biophys. Acta* 1558, 63–69.
- (18) Spudich, J. L. (1998) Variations on a molecular switch: transport and sensory signalling by archaeal rhodopsins. *Mol. Microbiol.* 28, 1051–1058.
- (19) Kitajima-Ihara, T., Furutani, Y., Suzuki, D., Ihara, K., Kandori, H., Homma, M., and Sudo, Y. (2008) *Salinibacter* sensory rhodopsin: sensory rhodopsin I-like protein from a eubacterium. *J. Biol. Chem.* 283, 23533–23541.
- (20) Sudo, Y., Okada, A., Suzuki, D., Inoue, K., Irieda, H., Sakai, M., Fujii, M., Furutani, Y., Kandori, H., and Homma, M. (2009) Characterization of a signaling complex composed of sensory rhodopsin I and its cognate transducer protein from the eubacterium *Salinibacter ruber*. *Biochemistry* 48, 10136–10145.
- (21) Suzuki, D., Furutani, Y., Inoue, K., Kikukawa, T., Sakai, M., Fujii, M., Kandori, H., Homma, M., and Sudo, Y. (2009) Effects of chloride ion binding on the photochemical properties of *Salinibacter* sensory rhodopsin I. *J. Mol. Biol.* 392, 48–62.
- (22) Yagasaki, J., Suzuki, D., Ihara, K., Inoue, K., Kikukawa, T., Sakai, M., Fujii, M., Homma, M., Kandori, H., and Sudo, Y. (2010) Spectroscopic studies of a sensory rhodopsin I homologue from the archaeon *Halorarcula vallismortis*. *Biochemistry* 49, 1183–1190.
- (23) Sudo, Y., Iwamoto, M., Shimono, K., Sumi, M., and Kamo, N. (2001) Photo-induced proton transport of *pharaonis* phoborhodopsin (sensory rhodopsin II) is ceased by association with the transducer. *Biophys. J.* 80, 916–922.
- (24) Kandori, H., Shimono, K., Shichida, Y., and Kamo, N. (2002) Interaction of Asn105 with the retinal chromophore during photoisomerization of *pharaonis* phoborhodopsin. *Biochemistry* 41, 4554–4559.
- (25) Sudo, Y., Furutani, Y., Shimono, K., Kamo, N., and Kandori, H. (2003) Hydrogen bonding alteration of Thr-204 in the complex between *pharaonis* phoborhodopsin and its transducer protein. *Biochemistry* 42, 14166–14172.
- (26) Suzuki, D., Sudo, Y., Furutani, Y., Takahashi, H., Homma, M., and Kandori, H. (2008) Structural changes of *Salinibacter* sensory rhodopsin I upon formation of the K and M photointermediates. *Biochemistry* 47, 12750–12759.
- (27) Furutani, Y., Iwamoto, M., Shimono, K., Kamo, N., and Kandori, H. (2002) FTIR spectroscopy of the M photointermediate in *pharaonis* phoborhodopsin. *Biophys. J.* 83, 3482–3489.
- (28) Iwamoto, M., Sudo, Y., Shimono, K., Araiso, T., and Kamo, N. (2005) Correlation of the O-intermediate rate with the pKa of Asp-75 in the dark, the counterion of the Schiff base of Pharaonis phoborhodopsin (sensory rhodopsin II). *Biophys. J.* 88, 1215–1223.
- (29) Rath, P., Spudich, E., Neal, D. D., Spudich, J. L., and Rothschild, K. J. (1996) Asp76 is the Schiff base counterion and proton acceptor in

the proton-translocating form of sensory rhodopsin I. *Biochemistry* 35, 6690–6696.

(30) Furutani, Y., Takahashi, H., Sasaki, J., Sudo, Y., Spudich, J. L., and Kandori, H. (2008) Structural changes of sensory rhodopsin I and its transducer protein are dependent on the protonated state of Asp76. *Biochemistry* 47, 2875–2883.

(31) Bousché, O., Spudich, E. N., Spudich, J. L., and Rothschild, K. J. (1991) Conformational changes in sensory rhodopsin I: similarities and differences with bacteriorhodopsin, halorhodopsin, and rhodopsin. *Biochemistry* 30, 5395–5400.

(32) Rath, P., Olson, K. D., Spudich, J. L., and Rothschild, K. J. (1994) The Schiff base counterion of bacteriorhodopsin is protonated in sensory rhodopsin I: spectroscopic and functional characterization of the mutated proteins D76N and D76A. *Biochemistry* 33, 5600–5606.

(33) Kandori, H. (2000) Role of internal water molecules in bacteriorhodopsin. *Biochim. Biophys. Acta* 1460, 177–191.

(34) Kandori, H., Kinoshita, N., Shichida, Y., Maeda, A., Needleman, R., and Lanyi, J. K. (1998) Cysteine S-H as a hydrogen-bonding probe in proteins. *J. Am. Chem. Soc.* 120, 5828–5829.

(35) Sudo, Y., Furutani, Y., Kandori, H., and Spudich, J. L. (2006) Functional importance of the interhelical hydrogen bond between Thr204 and Tyr174 of sensory rhodopsin II and its alteration during the signaling process. *J. Biol. Chem.* 281, 34239–34245.

(36) Sudo, Y., Furutani, Y., Iwamoto, M., Kamo, N., and Kandori, H. (2008) Structural changes in the O-decay accelerated mutants of *pharaonis* phororhodopsin. *Biochemistry* 47, 2866–2874.

(37) Garczarek, F., and Gerwert, K. (2006) Functional waters in intraprotein proton transfer monitored by FTIR difference spectroscopy. *Nature* 439, 109–112.

(38) Lorenz-Fonfria, V. A., Furutani, Y., and Kandori, H. (2008) Active internal waters in the bacteriorhodopsin photocycle. A comparative study of the L and m intermediates at room and cryogenic temperatures by infrared spectroscopy. *Biochemistry* 47, 4071–4081.

(39) Braiman, S., Mogi, T., Marti, T., Stern, L. J., Khorana, H. G., and Rothschild, K. J. (1988) Vibrational spectroscopy of bacteriorhodopsin mutants: light-driven proton transport involves protonation changes of aspartic acid residues 85, 96, and 212. *Biochemistry* 27, 8516–8520.

(40) Sudo, Y., Furutani, Y., Wada, A., Ito, M., Kamo, N., and Kandori, H. (2005) Steric constraint in the primary photoproduct of an archaeal rhodopsin from regiospecific perturbation of C-D stretching vibration of the retinyl chromophore. *J. Am. Chem. Soc.* 127, 16036–16037.

(41) Ito, M., Sudo, Y., Furutani, Y., Okitsu, T., Wada, A., Homma, M., Spudich, J. L., and Kandori, H. (2008) Steric constraint in the primary photoproduct of sensory rhodopsin II is a prerequisite for light-signal transfer to HtrII. *Biochemistry* 47, 6208–6215.

(42) Lanyi, J. K. (2004) X-ray diffraction of bacteriorhodopsin photocycle intermediates. *Mol. Membr. Biol.* 21, 143–150.

(43) Lanyi, J. K. (2006) Proton transfers in the bacteriorhodopsin photocycle. *Biochim. Biophys. Acta* 1757, 1012–1018.

(44) Sineshchekov, O. A., Sasaki, J., Phillips, B. J., and Spudich, J. L. (2008) A Schiff base connectivity switch in sensory rhodopsin signaling. *Proc. Natl. Acad. Sci. U.S.A.* 105, 16159–16164.

(45) Sineshchekov, O. A., Sasaki, J., Wang, J., and Spudich, J. L. (2010) Attractant and repellent signaling conformers of sensory rhodopsin-transducer complexes. *Biochemistry* 49, 6696–6704.

(46) Kim, S.-H., Wang, W., and Kim, K. K. (2002) Dynamic and clustering model of bacterial chemotaxis receptors: structural basis for signaling and high sensitivity. *Proc. Natl. Acad. Sci. U.S.A.* 99, 11611–11615.